

Pillar[4]pyridinium. A Square-Shaped Molecular Box

Sandra Kosiorek,^a Bartłomiej Rosa,^a Tomasz Boinski,^b Helena Butkiewicz,^a Marek P. Szymański,^b Oksana Danylyuk,^a Agnieszka Szumna,^{b*} and Volodymyr Sashuk^{a*}

^a Institute of Physical Chemistry, Polish Academy of Sciences, Kasprzaka 44/52, 01-224 Warsaw, Poland

^b Institute of Organic Chemistry, Polish Academy of Sciences, Kasprzaka 44/52, 01-224 Warsaw, Poland

E-mail: aszumna@icho.edu.pl, vsashuk@ichf.edu.pl

Supporting Information

Table of contents

1. Materials, instrumentation and methods	1
2. Synthesis	2
3. Characterization and properties	3
4. Binding studies	6
5. Computations	8
6. References	20

1. Materials, instrumentation and methods

All chemicals were purchased as reagent grade from commercial suppliers (Sigma-Aldrich, AlfaAesar, Fluorochem) and used without further purification. The solvents used (*Merck, ChemPur, PoCh*) were of analytical grade quality. DMSO was dried over alumina and calcium hydride, distilled under argon and then stored over molecular sieves. Deionized water (18.3 MΩ·cm) was obtained from Milli-Q station. NMR solvents and tubes were purchased from Armar Chemicals. Quartz cuvettes were purchased from Hellma Analytics. 4-(Bromomethyl)pyridine hydrobromide was synthesized according to literature procedure.¹

NMR spectra were recorded on Bruker (400 MHz) instrument. The chemical shifts (δ) are given in ppm relative to TMS, coupling constants are (J) in Hz. NMR data were analyzed using MestReNova Software. MS spectra were recorded on Maldi SYNAPT G2-S HDMS (Waters) spectrometer. UV-Vis spectra were recorded on Evolution220 spectrophotometer from Thermo Scientific. X-ray data were collected at 100 K on a SuperNova Agilent diffractometer using $\text{CuK}\alpha$ radiation ($\lambda = 1.54184 \text{ \AA}$) and $\text{MoK}\alpha$ radiation ($\lambda = 0.71073 \text{ \AA}$). The data were processed with *CrysAlisPro* (Agilent Technologies, *CrysAlisPro*, Version 1.171.35.21b). Structures were solved by direct methods and refined using *SHELXL-97*.² CCDC 1571841 and 1571842 contain the supplementary crystallographic data for this paper. These data are provided free of charge by The Cambridge Crystallographic Data Centre. Quantum chemical calculations were performed within the density functional theory (DFT) using the Gaussian 09 program suite.^[3] The geometry was taken from the crystal structure of P[4]P and optimized with the B3LYP functional, using the 6-31+g(d) basis set. PCM (polarized continuum model) solvent effects were considered within the CPCM to model the interaction with the solvent. Molecular orbitals and electrostatic potential maps were displayed using the GaussView program.^[4]

2. Synthesis

4-(bromomethyl)pyridine hydrobromide (2.53 g, 10 mmol) was dissolved in boiling acetonitrile (100 mL). Then, NaHCO₃ (0.92 g, 11 mmol) was added. After 1h, the addition of NH₄PF₆ (1.63 g, 10 mmol) was followed. The mixture was kept at reflux for 48h. After that it was cooled to room temperature and brick-red precipitate was filtered off. 100 mg of the crude residue was dissolved in 3 mL of 1M solution of KBr in water and boiled until the complete dissolution. Then, the resulting brown solution was allowed to cool slowly to ambient temperature. White solid was filtered off and recrystallized from distilled water to afford the pure P[4]P·(PF₆)₄. Brown filtrate was evaporated to dryness by rotary evaporation and recrystallized from 1M solution of KI in water. After slow cooling to room temperature an orange solid was appeared, which was filtered off and recrystallized from distilled water to afford the pure P[4]P·(I)₄. With this work-up the total yield of P[4]P was about 40%. ¹H NMR (400 MHz, 1M Na₂SO₄ in D₂O, P[4]P·(PF₆)₄): δ 9.25 (d, *J* = 6.6 Hz, 8H), 8.45 (d, *J* = 6.6 Hz, 8H), 6.23 (s, 8H). ¹³C NMR (100 MHz, 1M Na₂SO₄ in D₂O): δ 153.0, 146.0, 130.2, 62.5. For ion exchange, P[4]P·(PF₆)₄ was dissolved in hot water followed by addition of saturated aqueous solution of NaNTf₂ to give P[4]P·(NTf₂)₄. The white precipitate was collected by centrifugation, washed with water and dried. Afterwards, P[4]P·(NTf₂)₄ was dissolved in acetonitrile and 12N HCl solution was added causing the precipitation of P[4]P·(Cl)₄. Again, the precipitate was isolated using centrifuge, rinsed with acetonitrile and dried.

Reaction conditions	Observation
<i>Type of substrate:</i> 4-(chloromethyl)pyridine hydrochloride 4-(bromomethyl)pyridine hydrobromide	The reaction was faster for 4-(bromomethyl)pyridine hydrobromide.
<i>Type of base:</i> DBU, sodium hydrocarbonate, pyridine, triethylamine	The reaction was more selective in the presence DBU and sodium hydrocarbonate (NaHCO ₃).
<i>Amount of base:</i> 1-4 eq.	The highest yield was obtained using 1.1 eq. of DBU and NaHCO ₃ . Two and more eq. of DBU and NaHCO ₃ caused the formation of oligomeric products only.
<i>Solvent:</i> DMF, water, acetonitrile, nitromethane, acetone	The product was formed only in acetonitrile, nitromethane and acetone. The highest yield was obtained using acetonitrile (in the presence of NaHCO ₃).
<i>Additives:</i> Tetrabutylammonium chloride, bromide and iodide	Chloride and bromide salts had almost no influence on the reaction course, while in the presence of iodide the decomposition of the product occurred.

Table 1. Optimization of reaction conditions.

3. Characterization and properties

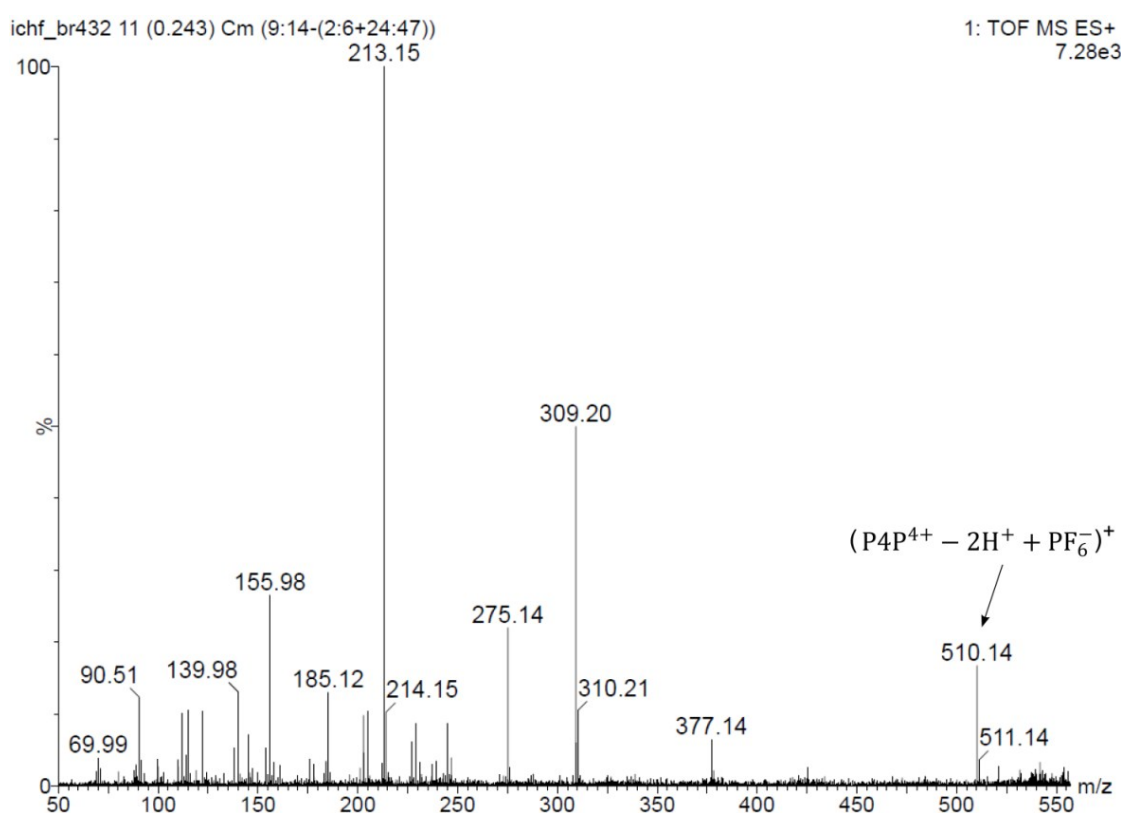


Figure S1. Mass spectrum of P[4]P·(PF₆)₄ under electrospray ionization.

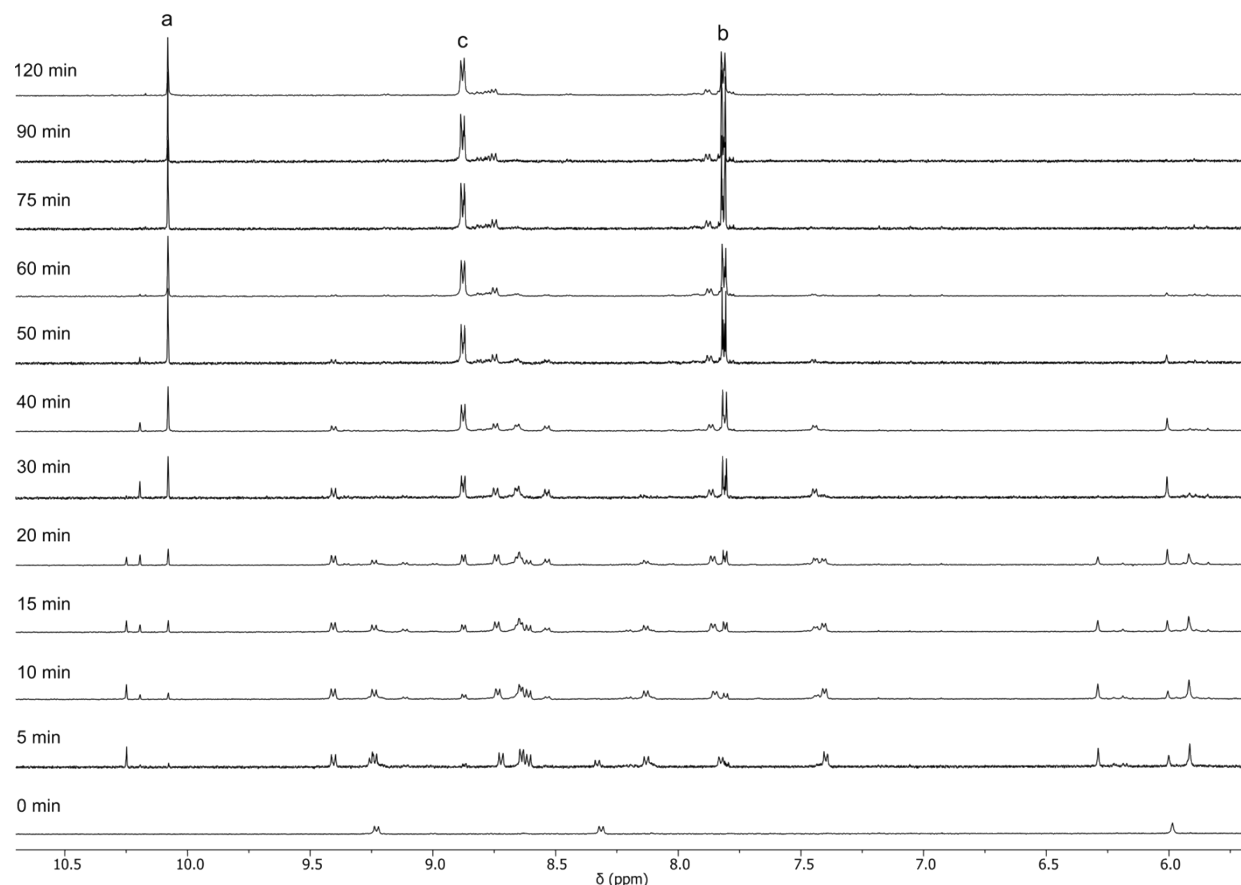
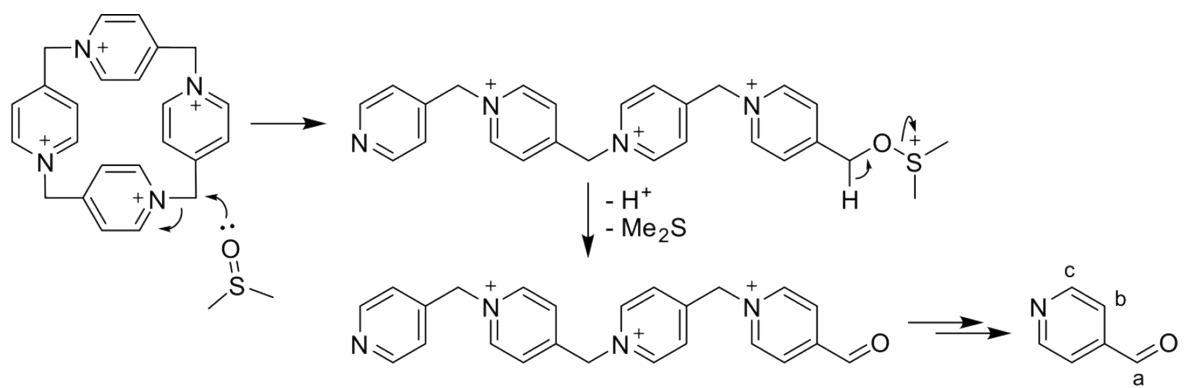


Figure S2. Plausible mechanism and time-resolved ${}^1\text{H}$ NMR spectra of degradation of $\text{P}[4]\text{P}\cdot(\text{PF}_6)_4$ in hot $\text{DMSO}-d_6$ (120°C).

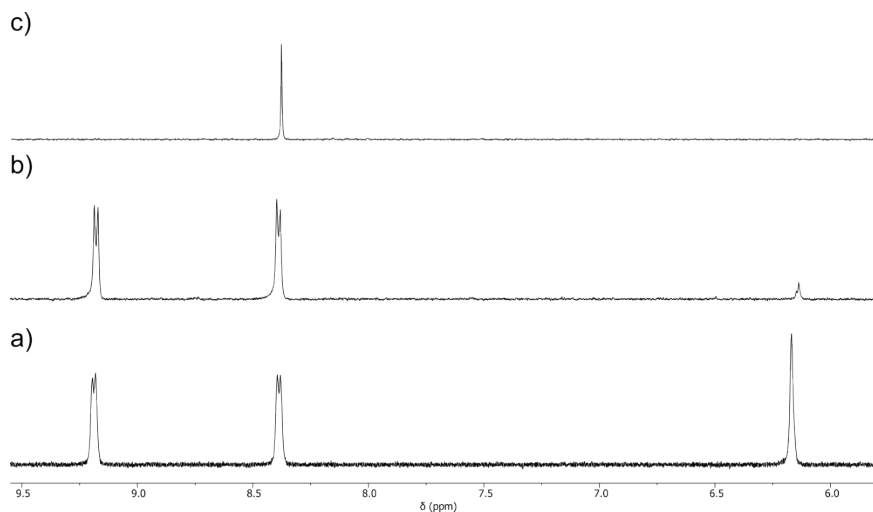


Figure S3. ^1H NMR spectra of $\text{P}[4]\text{P}\cdot(\text{PF}_6)_4$ in $\text{D}_2\text{O}-\text{CD}_3\text{CN}$ mixture: a) $\text{pD}=7$, 0h; b) $\text{pD}=7$, 24h; c) $\text{pD}=10$, 0h.

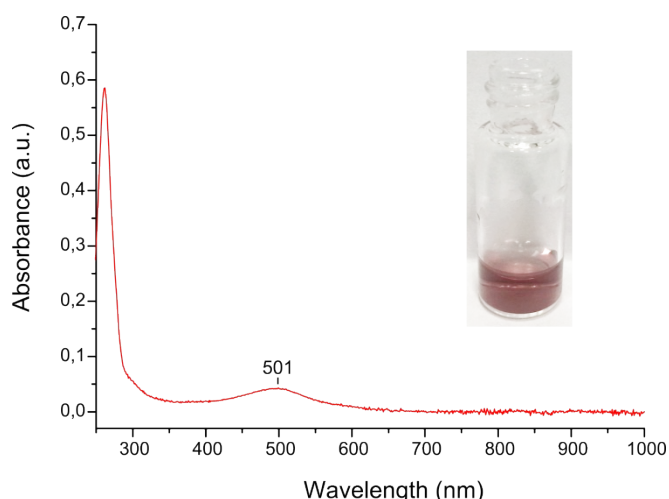


Figure S4. UV-Vis spectrum and photograph of alkalized $\text{P}[4]\text{P}\cdot(\text{PF}_6)_4$ aqueous solution.

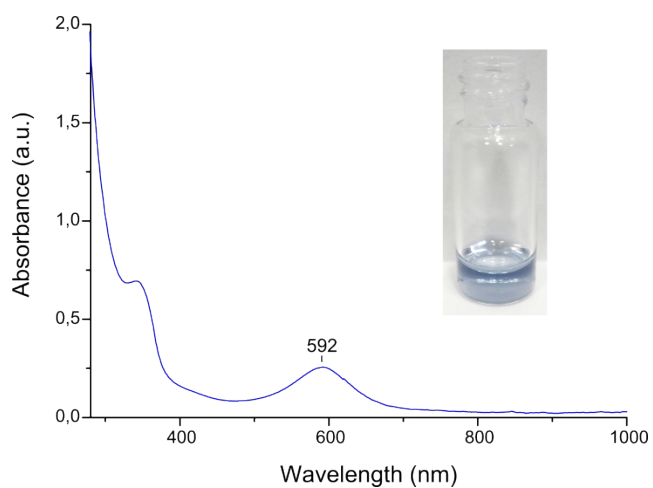


Figure S5. UV-Vis spectrum and photograph of $\text{P}[4]\text{P}\cdot(\text{PF}_6)_4$ in hot DMSO.

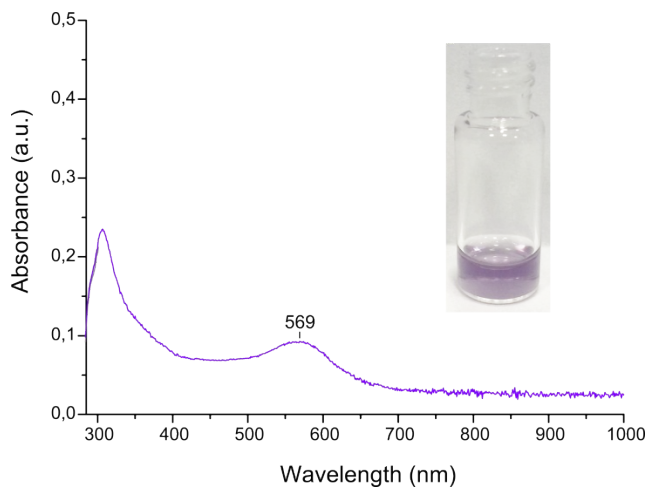


Figure S6. UV-Vis spectrum and photograph of $\text{P}[4]\text{P}\cdot(\text{PF}_6)_4$ in DMF after heating with SnCl_2 .

4. Binding studies

Titration was carried out in D_2O ($T = 298 \text{ K}$) by adding a solution of $\text{P}[4]\text{P}\cdot(\text{Cl})_4$ and TBAF (at 29,827 mM and 2,465 mM, respectively) to 2,465 mM solution of TBAF. ^{19}F NMR spectra were recorded after each addition (Figure S7). The experiment was repeated three times. Fitting procedure was performed using HypNMR software. A steep slope of the titration curve indicates formation of higher complexes. This was confirmed by the failure to fit the experimental data to binding models with low stoichiometry (Figures S8-S9). The best fit was obtained for a mixture of HG , HG_2 , HG_3 and HG_4 complexes.

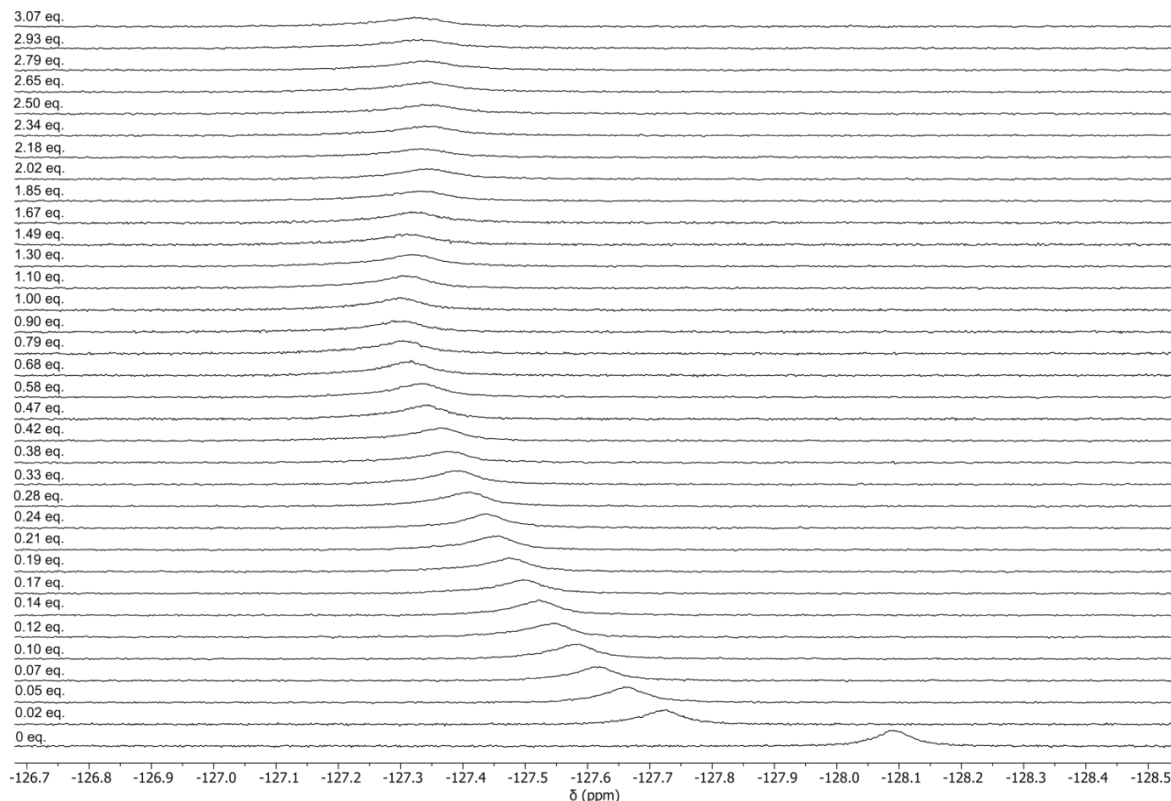


Figure S7. ^{19}F NMR spectra of fluoride with an increasing amount of $\text{P}[4]\text{P}$ in D_2O

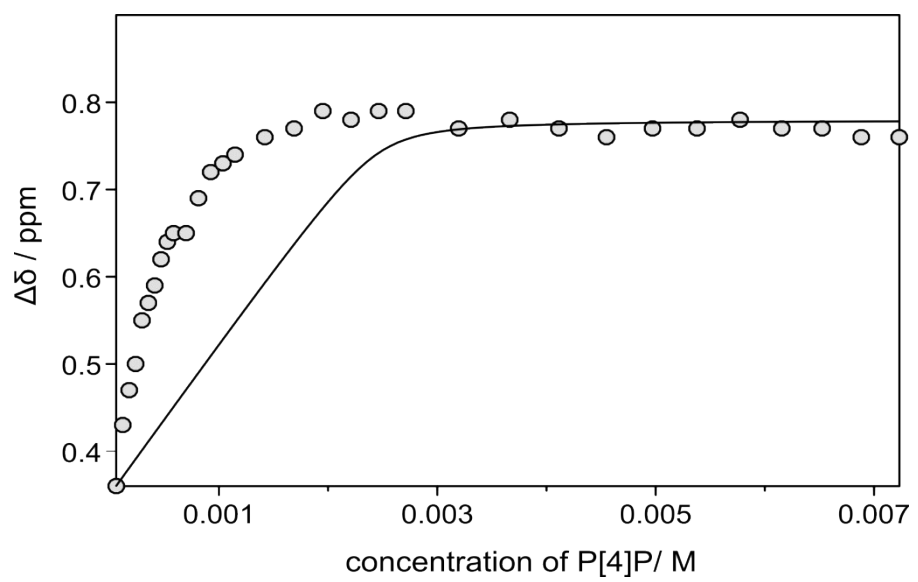


Figure S8. Experimental data fitted to a 1:1 binding model.

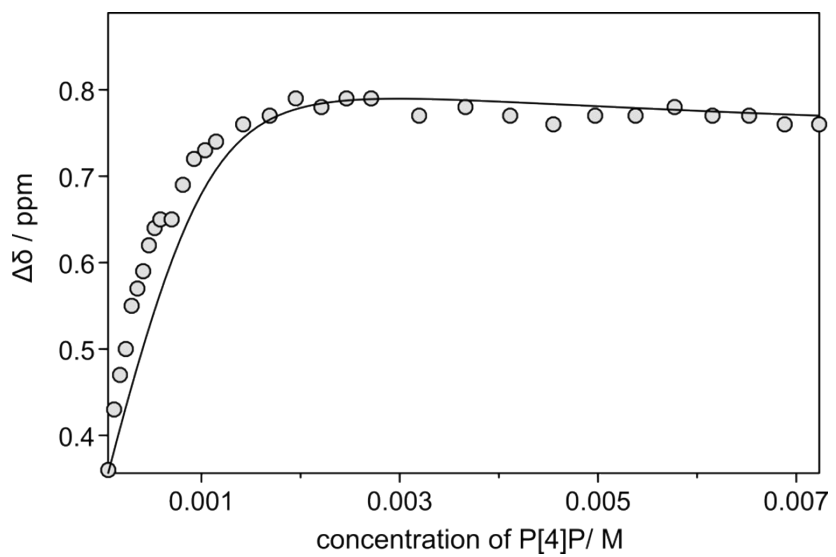


Figure S9. Experimental data fitted to 1:1 and 1:2 binding models.

5. Computations

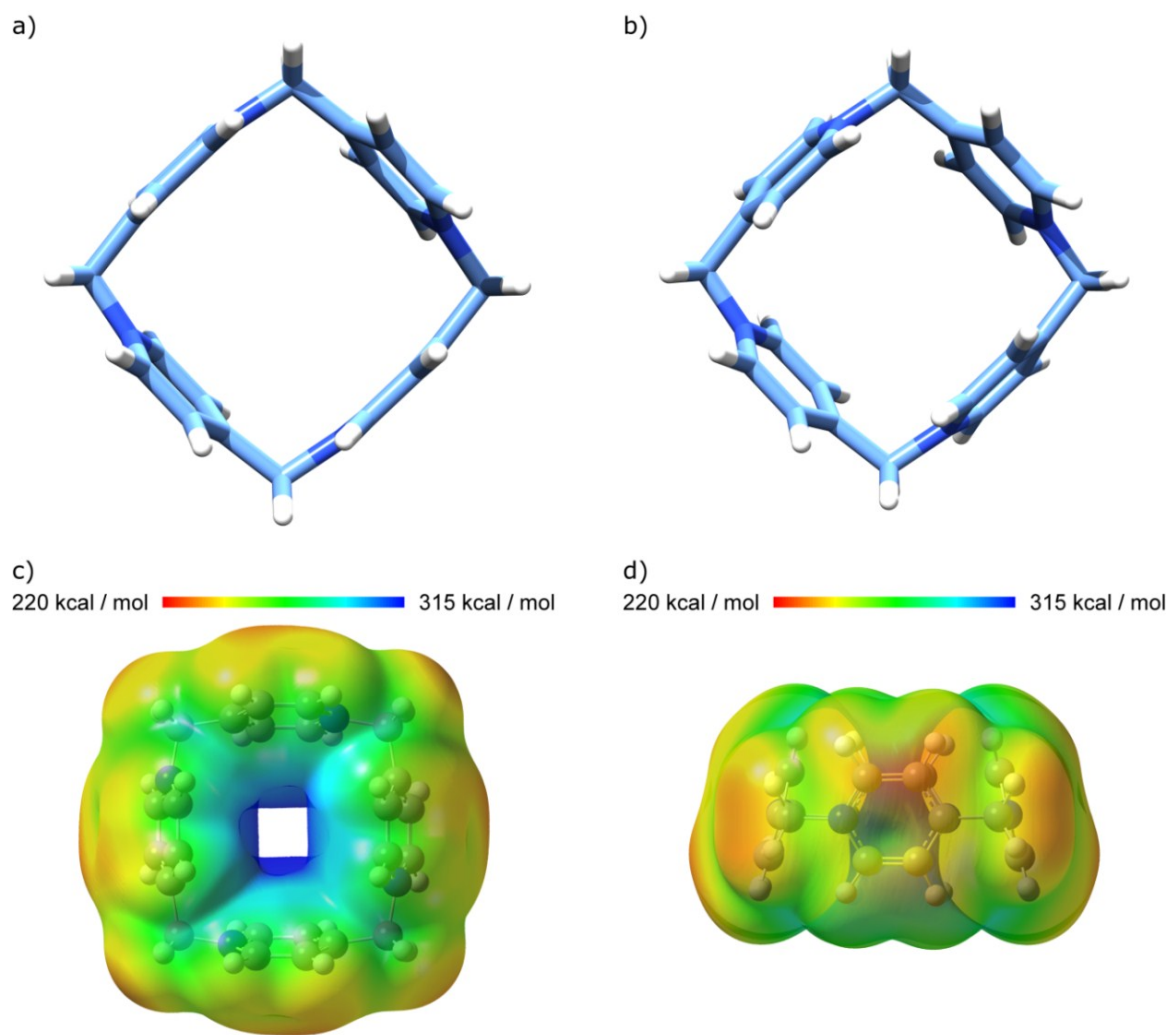


Figure S10. Structure of $\text{P}[4]\text{P}^{4+}$ before (a) and after (b) optimization. Electrostatic potential maps of $\text{P}[4]\text{P}^{4+}$, top (c) and side (d) view.

C	-0.48702800	3.36115100	0.03516300	C	2.79990200	0.97105800	-1.22493000
N	-2.84342600	1.90531800	0.06137300	H	2.88754100	0.43679200	-2.16397400
C	-3.96214000	0.90960600	0.03069900	C	2.07147700	2.14472700	-1.21185900
C	-2.14472700	2.07147700	1.21185900	H	1.58716500	2.53342100	-2.09851100
H	-2.53342100	1.58716500	2.09851100	H	1.05027800	4.56348000	-0.92857500
C	-0.97105800	2.79990200	1.22493000	H	1.12985500	4.58000300	0.83991500
H	-0.43679200	2.88754100	2.16397400	H	-4.56348000	1.05027800	0.92857500
C	0.90960600	3.96214000	-0.03069900	H	-4.58000300	1.12985500	-0.83991500
N	1.90531800	2.84342600	-0.06137300	C	-2.45996300	2.53398300	-1.07399100
C	3.36115100	0.48702800	-0.03516300	H	-3.08941000	2.40628200	-1.94550200
C	3.96214000	-0.90960600	0.03069900	C	-1.28810200	3.27422300	-1.10813700

H	-1.00370300	3.74420000	-2.04287400	H	3.08941000	-2.40628200	-1.94550200
H	4.58000300	-1.12985500	-0.83991500	C	1.28810200	-3.27422300	-1.10813700
H	4.56348000	-1.05027800	0.92857500	H	1.00370300	-3.74420000	-2.04287400
C	3.27422300	1.28810200	1.10813700	H	-1.05027800	-4.56348000	-0.92857500
H	3.74420000	1.00370300	2.04287400	H	-1.12985500	-4.58000300	0.83991500
C	2.53398300	2.45996300	1.07399100	N	-1.90531800	-2.84342600	-0.06137300
H	2.40628200	3.08941000	1.94550200	C	-3.36115100	-0.48702800	-0.03516300
C	0.48702800	-3.36115100	0.03516300	C	-2.79990200	-0.97105800	-1.22493000
N	2.84342600	-1.90531800	0.06137300	H	-2.88754100	-0.43679200	-2.16397400
C	2.14472700	-2.07147700	1.21185900	C	-2.07147700	-2.14472700	-1.21185900
H	2.53342100	-1.58716500	2.09851100	H	-1.58716500	-2.53342100	-2.09851100
C	0.97105800	-2.79990200	1.22493000	C	-3.27422300	-1.28810200	1.10813700
H	0.43679200	-2.88754100	2.16397400	H	-3.74420000	-1.00370300	2.04287400
C	-0.90960600	-3.96214000	-0.03069900	C	-2.53398300	-2.45996300	1.07399100
C	2.45996300	-2.53398300	-1.07399100	H	-2.40628200	-3.08941000	1.94550200

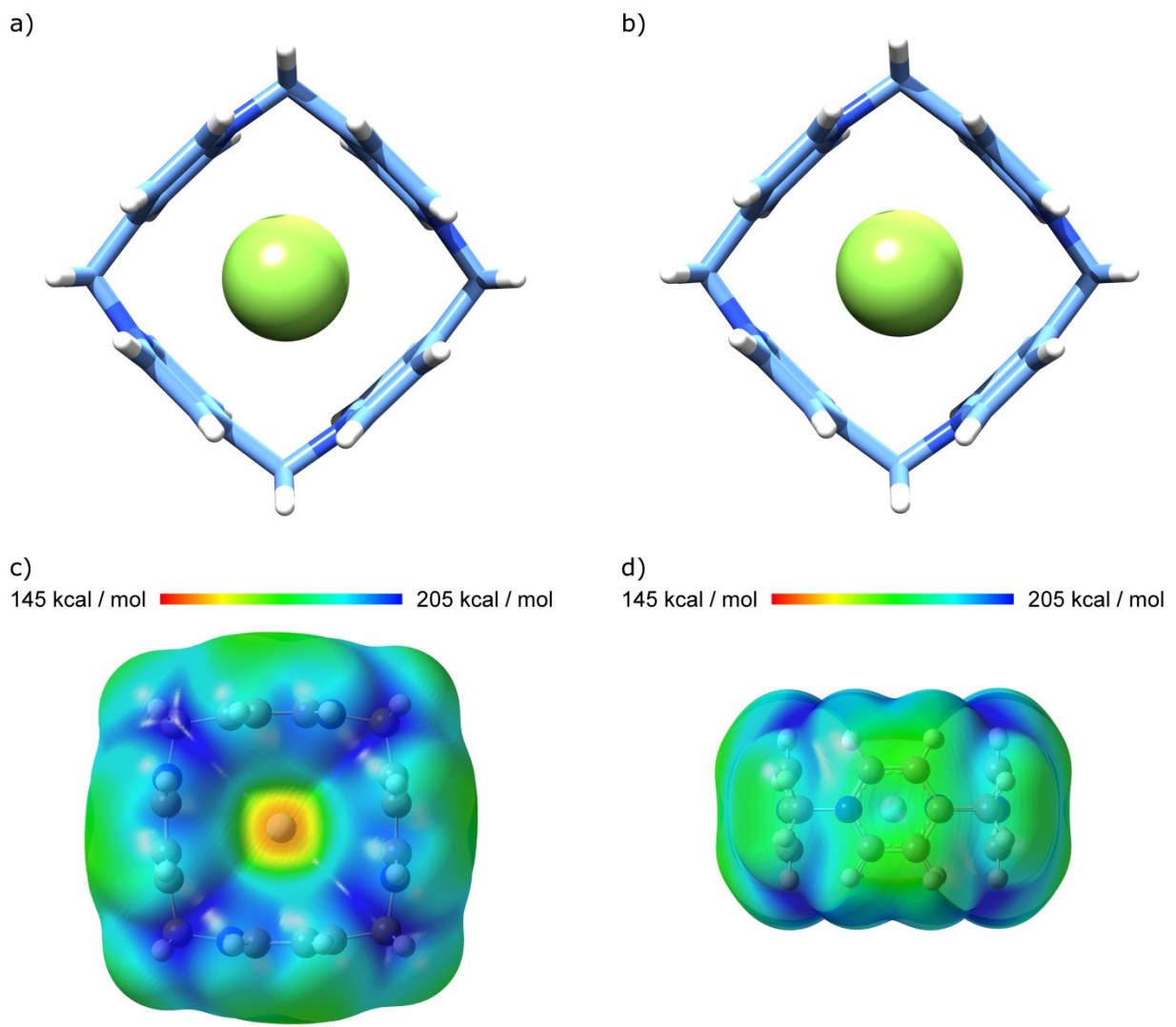


Figure S11. Structure of $\text{P}[4]\text{P}^{4+}\cdot\text{F}$ complex before (a) and after (b) optimization. Electrostatic potential maps of $\text{P}[4]\text{P}^{4+}\cdot\text{F}$, top (c) and side (d) view.

C	2.90774400	1.74436500	-0.01047200	C	2.19261400	-2.36439100	-1.19746600
N	0.65916400	3.35491600	0.01774000	H	1.91004300	-2.78289400	-2.15686700
C	-0.68945400	4.00143200	0.03107800	C	2.98679000	-1.23279300	-1.18623800
C	1.23311000	2.98754700	1.18641300	H	3.32552700	-0.75431900	-2.09612800
H	0.75503100	3.32688800	2.09628800	H	4.61450600	0.75689400	-0.92925600
C	2.36461400	2.19320200	1.19762600	H	4.65229200	0.75782300	0.84065000
H	2.78362900	1.91130200	2.15700400	H	-0.75691200	4.61468000	0.92957500
C	4.00119500	0.68938900	-0.03080500	H	-0.75789700	4.65258400	-0.84033700
N	3.35478000	-0.65928200	-0.01755000	C	1.22687500	3.02041500	-1.16381200
C	1.74445100	-2.90801400	0.01064700	H	0.74506900	3.38578800	-2.06151200
C	0.68941600	-4.00139100	0.03097200	C	2.35702700	2.22516000	-1.20257400

H	2.77133800	1.96743300	-2.17059600	C	-2.35741300	-2.22561900	-1.20274300
H	0.75783300	-4.65249200	-0.84048200	H	-2.77194900	-1.96828400	-2.17077400
H	0.75678300	-4.61469800	0.92943400	H	-4.61458100	-0.75679400	-0.92954000
C	2.22584800	-2.35773100	1.20271200	H	-4.65241500	-0.75781800	0.84037800
H	1.96863400	-2.77242000	2.17071300	N	-3.35474400	0.65922300	-0.01769600
C	3.02099200	-1.22747800	1.16396000	C	-1.74441800	2.90797400	0.01066100
H	3.38676700	-0.74594900	2.06165000	C	-2.19270100	2.36450100	-1.19748400
C	-2.90788100	-1.74440400	-0.01070300	H	-1.91026000	2.78315000	-2.15686000
N	-0.65918000	-3.35479800	0.01761000	C	-2.98691600	1.23291800	-1.18634400
C	-1.23286400	-2.98698700	1.18627400	H	-3.32575400	0.75457400	-2.09626500
H	-0.75452600	-3.32587000	2.09618200	C	-2.22564000	2.35747800	1.20269600
C	-2.36442000	-2.19274100	1.19743800	H	-1.96829900	2.77200800	2.17073200
H	-2.78308400	-1.91031700	2.15681400	C	-3.02078700	1.22722900	1.16385900
C	-4.00130100	-0.68940300	-0.03106300	H	-3.38644800	0.74558000	2.06152800
C	-1.22716600	-3.02077400	-1.16392000	F	0.00045300	-0.00040600	-0.00154300
H	-0.74551700	-3.38638800	-2.06160600				

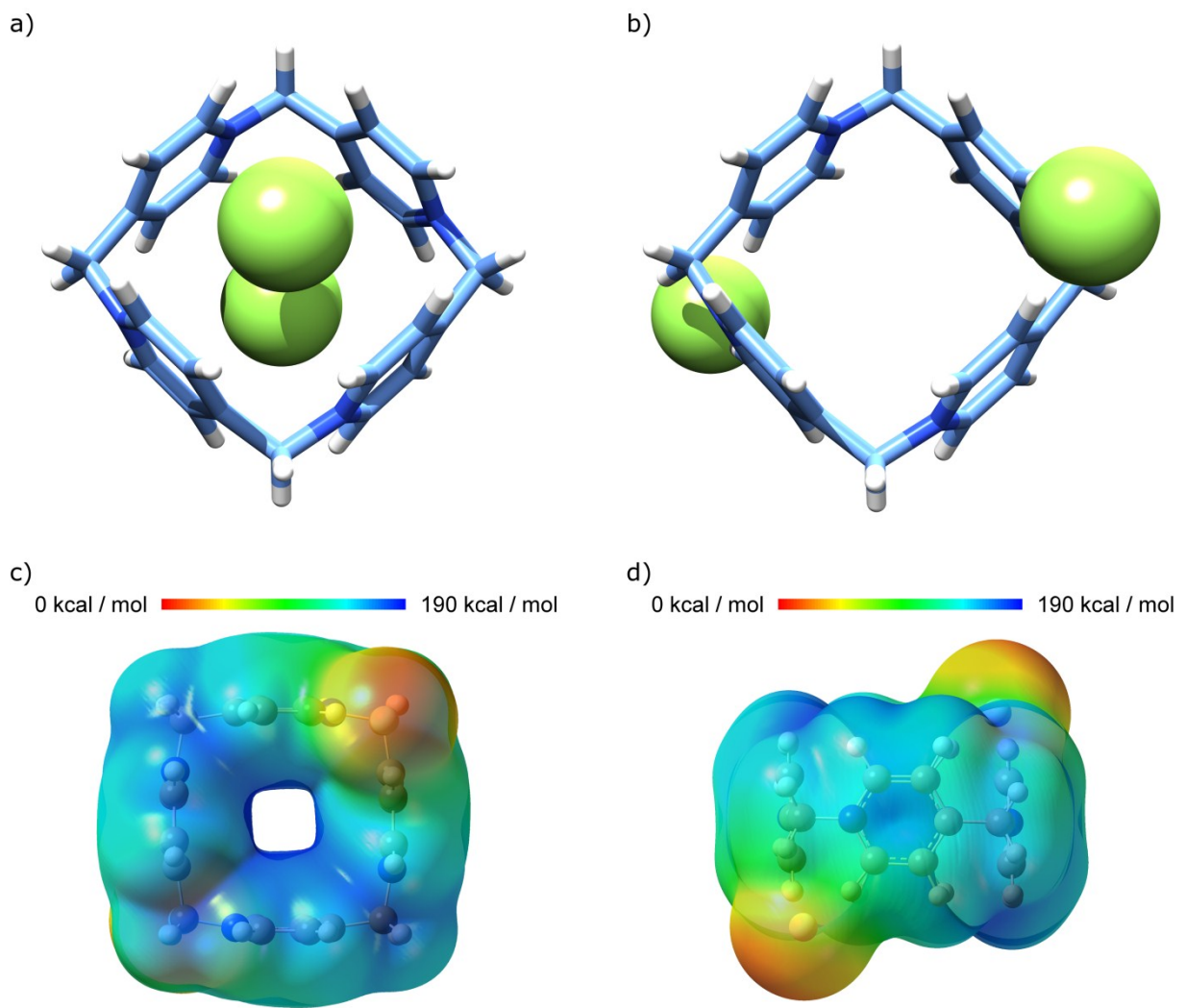


Figure S12. Structure of $\text{P}[4]\text{P}^{4+}\cdot\text{F}_2$ complex before (a) and after (b) optimization. Electrostatic potential maps of $\text{P}[4]\text{P}^{4+}\cdot\text{F}_2$, top (c) and side (d) view.

C	-1.26700000	3.14900000	-0.24100000	C	2.79700000	1.77400000	-0.67500000
N	-3.14500000	1.15900000	-0.61900000	H	3.32900000	1.34900000	-1.53400000
C	-3.97200000	-0.07900000	-0.78500000	C	1.82400000	2.74200000	-0.84200000
C	-2.92000000	1.61900000	0.63700000	H	1.55300000	3.13000000	-1.81500000
H	-3.48400000	1.10900000	1.44100000	H	0.11500000	4.71000000	-0.87400000
C	-1.98700000	2.62700000	0.83800000	H	-0.22100000	4.70400000	0.86500000
H	-1.81200000	2.96500000	1.85300000	H	-4.73100000	-0.06300000	-0.00200000
C	-0.08000000	4.07200000	-0.01200000	H	-4.43800000	-0.04600000	-1.77000000
N	1.13500000	3.22700000	0.22200000	C	-2.54500000	1.72000000	-1.69600000
C	3.06400000	1.28500000	0.61200000	H	-2.81700000	1.33200000	-2.66900000
C	3.97500000	0.07900000	0.77600000	C	-1.60500000	2.72100000	-1.53300000

H	-1.13200000	3.13200000	-2.41700000	C	1.98400000	-2.63100000	-0.83500000	
H	4.72900000	0.06200000	-0.01200000	H	1.80600000	-2.97200000	-1.84900000	
H	4.44600000	0.04600000	1.75700000	H	0.22000000	-4.70900000	-0.85100000	
C	2.41900000	1.87800000	1.70300000	H	-0.11800000	-4.70500000	0.88800000	
H	2.62800000	1.58500000	2.72600000	N	-1.13500000	-3.22700000	-0.21700000	
C	1.45000000	2.84200000	1.48200000	C	-3.06200000	-1.28500000	-0.61600000	
H	0.89500000	3.30100000	2.28900000	C	-2.40900000	-1.87600000	-1.70500000	
C	1.26600000	-3.14800000	0.24800000	H	-2.61200000	-1.58200000	-2.72900000	
N	3.14600000	-1.15800000	0.61400000	C	-1.44200000	-2.84000000	-1.47800000	
C	2.54800000	-1.71500000	1.69500000	H	-0.88000000	-3.29700000	-2.28300000	
H	2.82200000	-1.32500000	2.66700000	C	-2.80400000	-1.77500000	0.67100000	
C	1.60700000	-2.71700000	1.53700000	H	-3.34000000	-1.35100000	1.52800000	
H	1.13400000	-3.12400000	2.42400000	C	-1.83100000	-2.74400000	0.84300000	
C	0.07800000	-4.07200000	0.02300000	H	-1.56700000	-3.13400000	1.81700000	
C	2.91800000	-1.62300000	-0.63900000	F	4.45300000	0.01600000	-2.35300000	
H	3.48000000	-1.11400000	-1.44500000	F		-4.45900000	-0.01800000	2.34700000

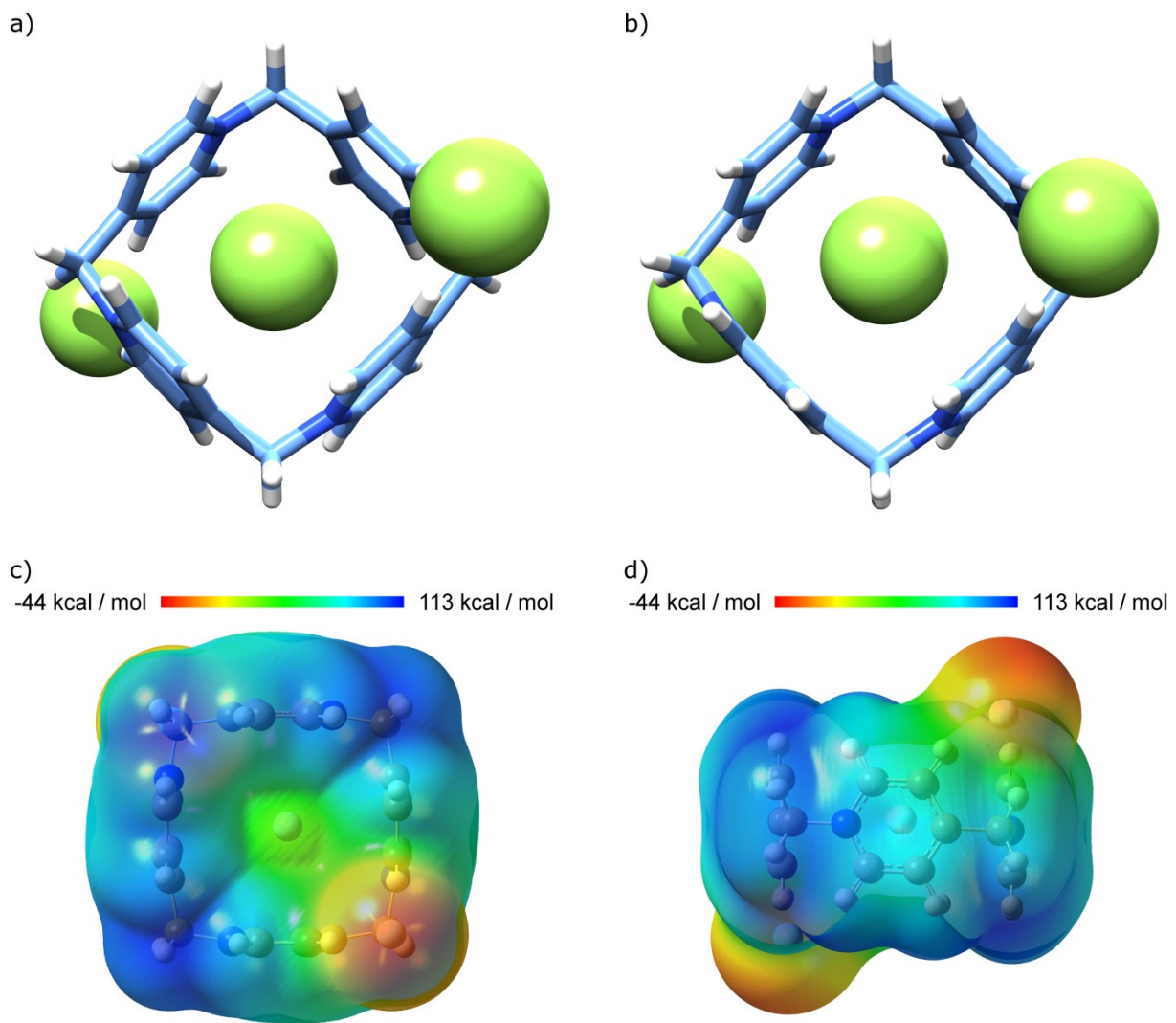


Figure S13. Structure of $\text{P}[4]\text{P}^{4+}\cdot\text{F}_3$ complex before (a) and after (b) optimization. Electrostatic potential maps of $\text{P}[4]\text{P}^{4+}\cdot\text{F}_3$, top (c) and side (d) view.

C	-1.30179000	3.13816600	-0.23297600	C	2.78103400	1.79815500	-0.66058900
N	-3.16552800	1.13835600	-0.62052200	H	3.31324900	1.37799300	-1.51970500
C	-3.97795200	-0.10752800	-0.79277500	C	1.79260700	2.74940800	-0.82806600
C	-2.93755600	1.58891400	0.63675100	H	1.50989400	3.12628700	-1.80265000
H	-3.49646400	1.07172700	1.43717300	H	0.07143900	4.70688700	-0.85953900
C	-2.01432200	2.60279300	0.84356000	H	-0.26582300	4.69420000	0.87880000
H	-1.83614700	2.93166600	1.86174200	H	-4.74394600	-0.09880100	-0.01641500
C	-0.11934900	4.06474800	0.00069300	H	-4.43700800	-0.07740400	-1.78105000
N	1.10188300	3.23202000	0.23367000	C	-2.57355600	1.71270600	-1.69299100
C	3.05407600	1.31584500	0.62491500	H	-2.84297400	1.32920100	-2.66885500
C	3.97129400	0.11595100	0.79153900	C	-1.64459100	2.72274600	-1.52561100

H	-1.17611600	3.14505300	-2.40770200	H	1.84285100	-2.95970700	-1.83081400
H	4.72953100	0.10443100	0.00755400	H	0.25648300	-4.69130000	-0.84175900
H	4.44103800	0.08859000	1.77483500	H	-0.08877900	-4.68712800	0.89517800
C	2.40572900	1.90495600	1.71553400	N	-1.10672300	-3.21828300	-0.21549700
H	2.62055600	1.61597500	2.73871900	C	-3.05758900	-1.30469700	-0.62139200
C	1.42351500	2.85368700	1.49336100	C	-2.37997300	-1.87074700	-1.70476300
H	0.86446200	3.30946900	2.30025900	H	-2.57058500	-1.56423000	-2.72749600
C	1.29428600	-3.13055200	0.26073600	C	-1.39522400	-2.81452500	-1.47337400
N	3.15595600	-1.12794200	0.63104400	H	-0.80808100	-3.24719600	-2.27312700
C	2.55244700	-1.68254100	1.70848800	C	-2.81018900	-1.80465000	0.66321000
H	2.81659300	-1.28380200	2.67977300	H	-3.36045800	-1.39817400	1.51728100
C	1.62417300	-2.69296800	1.54987900	C	-1.82289200	-2.75580200	0.83770400
H	1.14512500	-3.09921600	2.43391100	H	-1.56355600	-3.15058700	1.81172800
C	0.10979400	-4.05356600	0.03031100	F	-4.50413800	-0.04689400	2.36339000
C	2.93494700	-1.59673500	-0.61911900	F	4.48199600	0.05407000	-2.36743800
H	3.49185200	-1.08774500	-1.42403300	F	0.09221300	-0.13442600	-0.16432600
C	2.01726800	-2.61709700	-0.81657600				

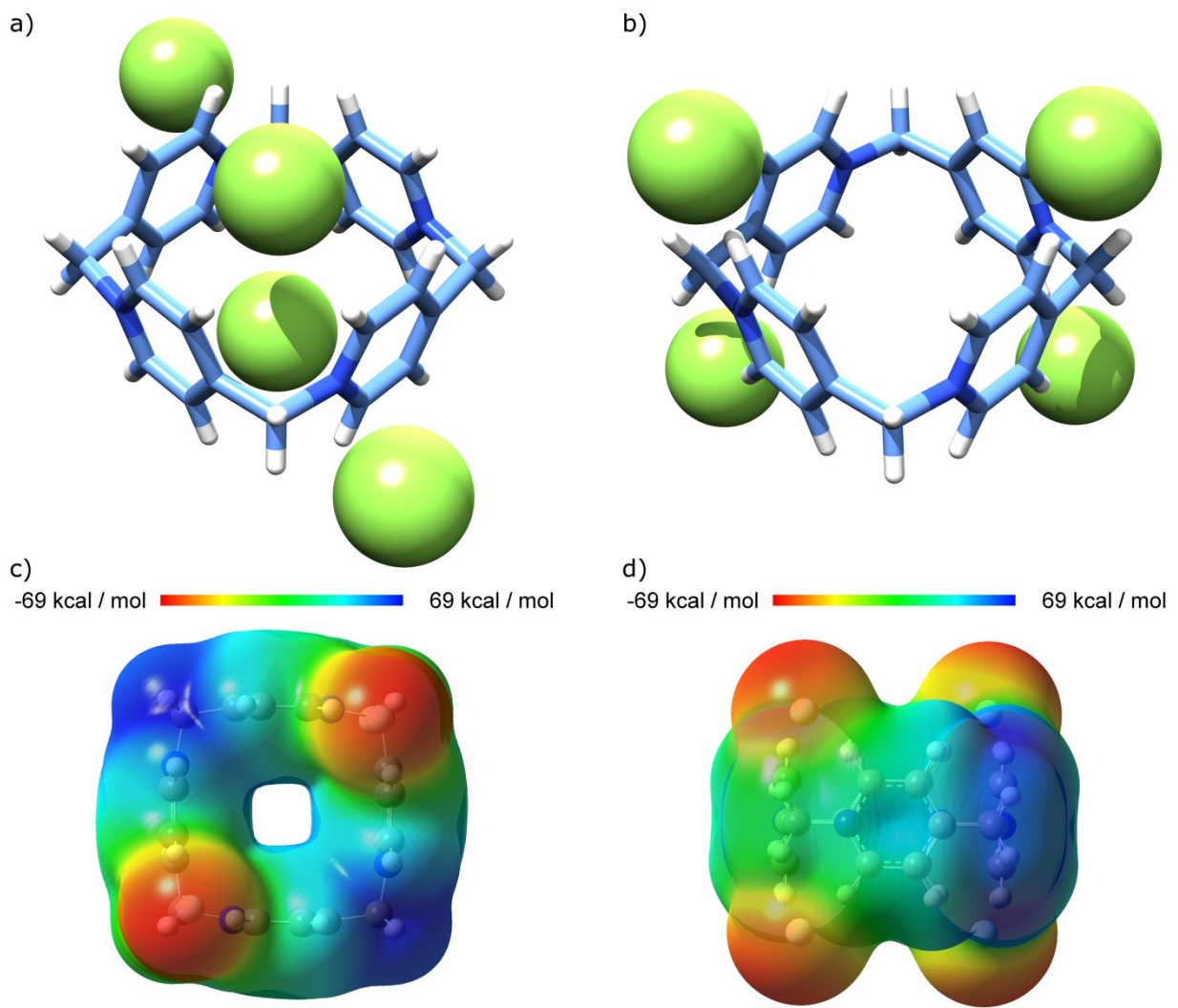


Figure S14. Structure of $\text{P}[4]\text{P}^{4+}\cdot\text{F}_4$ complex before (a) and after (b) optimization. Electrostatic potential maps of $\text{P}[4]\text{P}^{4+}\cdot\text{F}_4$, top (c) and side (d) view.

C	3.14899400	1.27005400	0.00000000	C	1.80016400	-2.66300600	-1.21021300
N	1.16775200	3.18378700	0.00000000	H	1.39967700	-3.03724700	-2.15779900
C	-0.05733400	4.04422800	0.00000000	C	2.77328700	-1.67977100	-1.17954600
C	1.66581500	2.76070700	1.18825400	H	3.19786700	-1.25196500	-2.07919700
H	1.17994800	3.17765300	2.08784400	H	4.70041700	0.02353600	-0.88522200
C	2.67155800	1.80595200	1.20237300	H	4.70041700	0.02353600	0.88522200
H	3.04353500	1.46575800	2.16286400	H	-0.02791400	4.65275200	0.90356500
C	4.06544500	0.05608600	0.00000000	H	-0.02791400	4.65275200	-0.90356500
N	3.21621100	-1.17591000	0.00000000	C	1.66581500	2.76070700	-1.18825400
C	1.26702700	-3.12622500	0.00000000	H	1.17994800	3.17765300	-2.08784400
C	0.05733400	-4.04422800	0.00000000	C	2.67155800	1.80595200	-1.20237300

H	3.04353500	1.46575800	-2.16286400	H	-3.04353500	-1.46575800	-2.16286400
H	0.02791400	-4.65275200	-0.90356500	H	-4.70041700	-0.02353600	-0.88522200
H	0.02791400	-4.65275200	0.90356500	H	-4.70041700	-0.02353600	0.88522200
C	1.80016400	-2.66300600	1.21021300	N	-3.21621100	1.17591000	0.00000000
H	1.39967700	-3.03724700	2.15779900	C	-1.26702700	3.12622500	0.00000000
C	2.77328700	-1.67977100	1.17954600	C	-1.80016400	2.66300600	-1.21021300
H	3.19786700	-1.25196500	2.07919700	H	-1.39967700	3.03724700	-2.15779900
C	-3.14899400	-1.27005400	0.00000000	C	-2.77328700	1.67977100	-1.17954600
N	-1.16775200	-3.18378700	0.00000000	H	-3.19786700	1.25196500	-2.07919700
C	-1.66581500	-2.76070700	1.18825400	C	-1.80016400	2.66300600	1.21021300
H	-1.17994800	-3.17765300	2.08784400	H	-1.39967700	3.03724700	2.15779900
C	-2.67155800	-1.80595200	1.20237300	C	-2.77328700	1.67977100	1.17954600
H	-3.04353500	-1.46575800	2.16286400	H	-3.19786700	1.25196500	2.07919700
C	-4.06544500	-0.05608600	0.00000000	F	0.01014500	3.91086200	3.21823300
C	-1.66581500	-2.76070700	-1.18825400	F	0.01014500	3.91086200	-3.21823300
H	-1.17994800	-3.17765300	-2.08784400	F	-0.01014500	-3.91086200	3.21823300
C	-2.67155800	-1.80595200	-1.20237300	F	-0.01014500	-3.91086200	-3.21823300

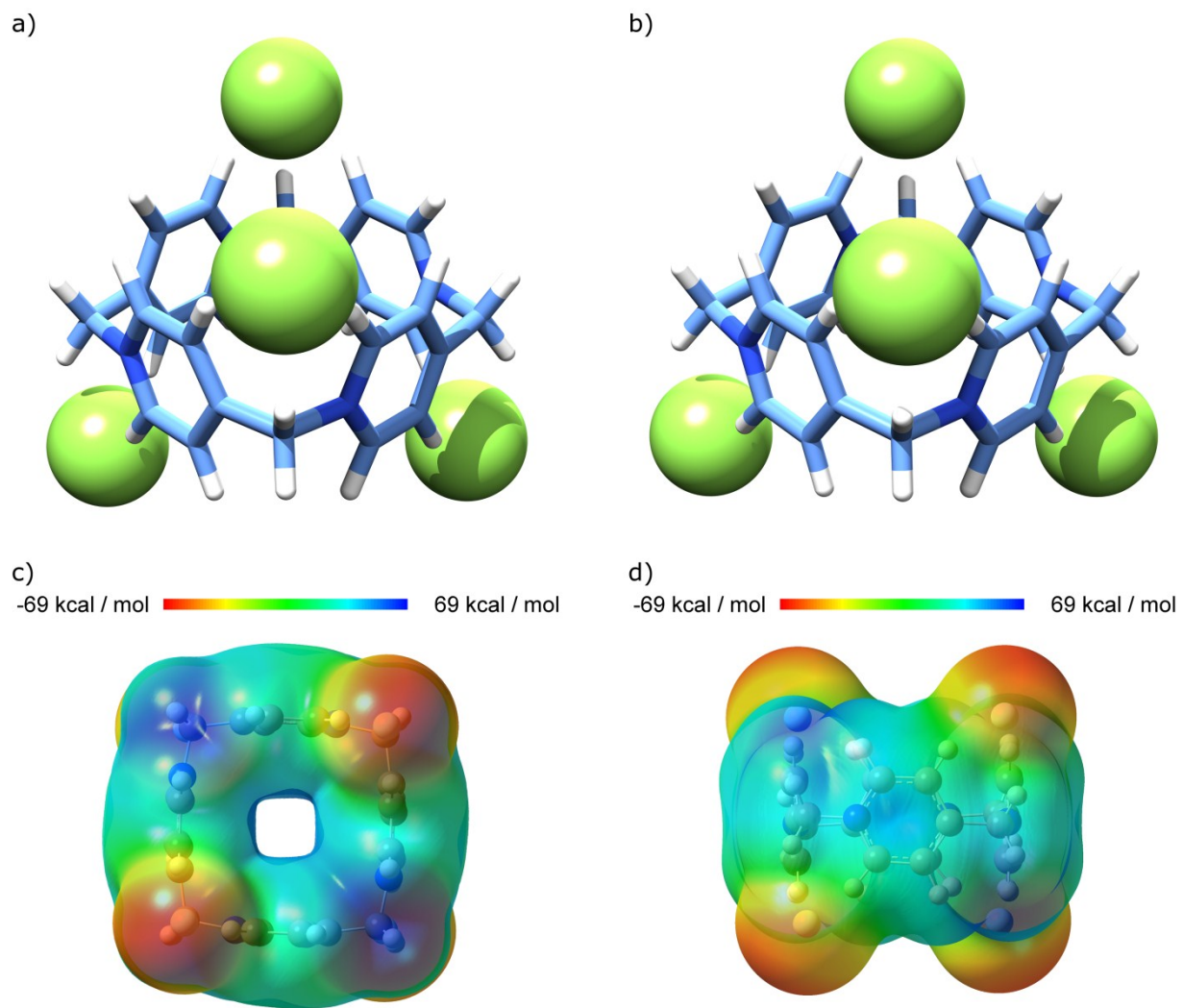


Figure S15. Alternative structure of $\text{P}[4]\text{P}^{4+}\cdot\text{F}_3$ complex before (a) and after (b) optimization. Electrostatic potential maps of $\text{P}[4]\text{P}^{4+}\cdot\text{F}_3$, top (c) and side (d) view.

C	-1.73100000	2.90500000	0.08600000	C	3.99400000	0.67300000	-0.15600000
N	-3.34100000	0.67300000	-0.08100000	C	2.31800000	2.26000000	-1.24000000
C	-3.99400000	-0.67300000	-0.15600000	H	2.70100000	2.03300000	-2.22900000
C	-3.06000000	1.18700000	1.14100000	C	1.18700000	3.06000000	-1.14100000
H	-3.46000000	0.62100000	2.00200000	H	0.62100000	3.46000000	-2.00200000
C	-2.26000000	2.31800000	1.24000000	H	-0.75300000	4.66400000	-0.70100000
H	-2.03300000	2.70100000	2.22900000	H	-0.72300000	4.55800000	1.08700000
C	-0.67300000	3.99400000	0.15600000	H	-4.66400000	-0.75300000	0.70100000
N	0.67300000	3.34100000	0.08100000	H	-4.55800000	-0.72300000	-1.08700000
C	2.90500000	1.73100000	-0.08600000	C	-2.93000000	1.28600000	-1.22000000

H	-3.24100000	0.83600000	-2.15500000	H	-0.83600000	-3.24100000	2.15500000
C	-2.12600000	2.40900000	-1.16600000	F	-4.14700000	-0.61000000	3.05600000
H	-1.76100000	2.89000000	-2.07900000	F	-0.61000000	4.14700000	-3.05600000
H	4.55800000	0.72300000	-1.08700000	F	4.14700000	0.61000000	3.05600000
H	4.66400000	0.75300000	0.70100000	F	0.61000000	-4.14700000	-3.05600000
C	2.40900000	2.12600000	1.16600000				
H	2.89000000	1.76100000	2.07900000				
C	1.28600000	2.93000000	1.22000000				
H	0.83600000	3.24100000	2.15500000				
C	1.73100000	-2.90500000	0.08600000				
N	3.34100000	-0.67300000	-0.08100000				
C	3.06000000	-1.18700000	1.14100000				
H	3.46000000	-0.62100000	2.00200000				
C	2.26000000	-2.31800000	1.24000000				
H	2.03300000	-2.70100000	2.22900000				
C	0.67300000	-3.99400000	0.15600000				
C	2.93000000	-1.28600000	-1.22000000				
H	3.24100000	-0.83600000	-2.15500000				
C	2.12600000	-2.40900000	-1.16600000				
H	1.76100000	-2.89000000	-2.07900000				
H	0.75300000	-4.66400000	-0.70100000				
H	0.72300000	-4.55800000	1.08700000				
N	-0.67300000	-3.34100000	0.08100000				
C	-2.90500000	-1.73100000	-0.08600000				
C	-2.31800000	-2.26000000	-1.24000000				
H	-2.70100000	-2.03300000	-2.22900000				
C	-1.18700000	-3.06000000	-1.14100000				
H	-0.62100000	-3.46000000	-2.00200000				
C	-2.40900000	-2.12600000	1.16600000				
H	-2.89000000	-1.76100000	2.07900000				
C	-1.28600000	-2.93000000	1.22000000				

6. References

- [1] Z. Liu, Q. Lin, Q. Huang, H. Liu, C. Bao, W. Zhang, X. Zhong, L. Zhu, *Chem. Commun.* **2011**, *47*, 1482-1484.
- [2] G. Sheldrick, *Acta Crystallogr. Sect. A* **2008**, *64*, 112-122.
- [3] Frisch MJ et al. (2009) Gaussian 09, Revision B.01. Gaussian, Inc., Wallingford CT.
- [4] Dennington R, Keith T, Millam J (2009) GaussView, Version 5, Semichem Inc., Shawnee Mission, KS.